Published in final edited form as:
Lasers Surg Med. 2015 January ; 47(1): 30–39. doi:10.1002/lsm.22307.

Dual Optical Modality Endoscopic Imaging of Cancer Development in the Mouse Colon

Molly R. Keenan, BS,
The University of Arizona, Department of Biomedical Engineering, 1657 E. Helen St., P.O. Box 210240, Tucson, AZ, 85721

Sarah J. Leung, PhD,
The University of Arizona, Department of Biomedical Engineering, 1657 E. Helen St., P.O. Box 210240, Tucson, AZ, 85721

Photini S. Rice, AAS,
The University of Arizona, Department of Biomedical Engineering, 1657 E. Helen St., P.O. Box 210240, Tucson, AZ, 85721

R. Andrew Wall, PhD, and
The University of Arizona, College of Optical Sciences, 1630 E. University Blvd, Tucson, AZ, 85721

Jennifer K. Barton, PhD
The University of Arizona, Department of Biomedical Engineering, 1657 E. Helen St., P.O. Box 210240, Tucson, AZ, 85721

The University of Arizona, College of Optical Sciences, 1630 E. University Blvd, Tucson, AZ, 85721

Abstract

Background and Objective—We utilize a miniature, dual-modality endoscope that combines fluorescence-based surface magnifying chromoendoscopy (SMC) and optical coherence tomography (OCT) to follow the anatomical changes that occur during adenoma development in the mouse colon.

Materials and Methods—Twenty-five mice were treated with the carcinogen azoxymethane (AOM) to induce tumor development in the distal colon, or were treated with saline as control, and were imaged over six months. OCT detects adenoma number with high sensitivity and specificity and can measure lesion size. In methylene blue-lavaged colons, SMC detects changes in the colonic crypts. SMC images of control mouse colons exhibit reticulated patterns of crypts of equal size, forming either a dot or honeycomb pattern.

Results—Images of AOM-treated colons show mild crypt irregularities even in grossly normal tissue. Images of small to medium adenoma exhibit larger crypts, more intense signal, and

Correspondence: Molly Keenan, The University of Arizona, Keating Building, 1657 E Helen Street, Tucson, AZ 85721, Cell: (508) 333 – 5314, mkeenan@email.arizona.edu.

irregular spacing whereas those of large adenoma have heterogeneous, intense signal and loss of crypt structure.

Conclusions—The combination of OCT and SMC permits the detection of neoplastic events from the earliest stages of crypt irregularities before gross tissue changes are noted, through to measuring the growth of protruding adenoma.

Introduction

Colon cancer is the third most frequently diagnosed cancer and third leading cause of cancer related deaths for men and women in the Unites States. When detected at an early, localized stage the 5-year survival rate is 90%, however, only 39% of cancers are found at this stage(1). Colonoscopy is the most commonly used technique to screen for colon cancer. Presently, this technique is forward-viewing and is most sensitive to detecting adenoma that protrude into the lumen. Because this method uses white light to scan for morphological changes in the colon, small, flat or low contrast lesions can be missed(2, 3). To improve survival rate, it is imperative to catch lesions at an early stage before they become invasive, thus making colonoscopy a more effective screening modality.

To identify the morphological characteristics of the earliest stages of colorectal cancer, a mouse model can be used (4). Mouse models have been used to assess the effect of diet (5), preventive, and therapeutic drugs (6) on colon cancer. Current studies into cancer and inflammatory conditions of the colon generally involve the sacrifice of animals at intervals throughout the study for gross tissue and histological assessment. Considering mouse-to-mouse variation, this paradigm requires a large number of animals to be statistically relevant. Serial experimental colonoscopy in mice can be performed and lesions tracked in individual mice. Groups have successfully used pediatric cytoscopes (7) or miniature endoscopes such as ‘Coloview’ (8, 9). These methods, similar to those used in humans, insufflate the colon and use forward viewing endoscopes with wide fields of view to scan for polyps. The required procedure can be lengthy, require operator expertise, and does not automatically generate an image map of the entire colon.

Using methylene blue, which stains actively absorbing epithelium (10), in conjunction with magnifying endoscopy reportedly improves sensitivity for detection of flat or depressed lesions (11–13), and can detect aberrant crypt foci, potential precursors to adenoma, found in both mice (14) and humans(15). Uptake of methylene blue is further improved with the use of a mucolytic agent, such as N-acetylcysteine (10). Using magnifying colonoscopy Kudo, et al., created a six group classification of ‘pit pattern’ (16). The classifications differentiate between non-neoplastic and neoplastic lesions with good sensitivity (86.2%) and specificity (99.2%) (17), and can be used clinically to determine which lesions require removal(18).

Surface magnifying chromoendoscopy (SMC) is thus a proven procedure, capable of resolving colon mucosal structure in a mouse(8). Methylene blue, an FDA approved dye, is typically used as an absorber in white light reflectance imaging (19), but also has significant fluorescence emission in the red to near-infrared wavelengths. Detecting fluorescence emission rather than reflected light simplifies the optical design for miniature endoscopes, as

the same optical path can be used for both illumination and detection without excessive attention paid to backreflections in the optical path. Optical coherence tomography (OCT) derives its contrast from the innate structure (index of refraction changes) of the tissue, uses near-infrared wavelengths to enable reasonable depth penetration (~ 2 mm), and can be easily miniaturized (20). Our laboratory has shown that OCT is useful in mouse models of colon cancer, having the ability to detect adenoma with high accuracy and track adenoma formation over time (21). OCT can be used to image human colonic crypts (22), and while our system has the capability to resolve mouse colonic crypts, the limited contrast of the very small crypts in the mouse precludes reliable imaging with OCT. Therefore SMC is a complementary modality as it can visualize these structures with high resolution and contrast (23).

We have combined fluorescence-based SMC and OCT into an automated side-viewing rigid probe in order to study the natural history of colon cancer development in an AOM-treated mouse model. Image acquisition is automated, which enables generation of image maps from the fluorescence-based SMC and OCT data. SMC generates an 18x320 matrix of images that fully sample the surface of the colon and OCT generates an 8×5000 matrix that samples cross-sections of the colon up to 2mm deep, at 45° rotational increments around the circumference of the colon. SMC is sensitive to early changes in the colon crypt pattern and OCT can quantify epithelial thickening and measure the morphology of adenoma. By combining SMC with OCT, we can observe the time course of anatomical changes occurring during adenoma development.

Materials and Methods

System description

We have combined OCT and SMC into an endoscope previously described in detail (23). Briefly, the fluorescence-based SMC utilizes a 638nm laser diode as a light source, which can excite methylene blue fluorescence. Excitation light is coupled to the distal optics through a 30,000 element, 0.72mm clear aperture fiber bundle (IGN-08/30, Sumitomo Electric USA, Torrance, CA, USA), which has a core-to-core spacing of 4 μm, and is suitable for imaging the mouse colon crypts at 1:1 magnification. Emission light is relayed back through the same fiber bundle where it is split off with a dichroic beam splitter and imaged onto a CCD array. Images 720 μm in diameter are obtained at 4 μm lateral resolution.

The Fourier Domain OCT subsystem was also previously described in detail(24). A superluminescent diode source (Superlum, Moscow, Russia) was used with a center wavelength of 890 nm and a full width half maximum bandwidth of 150 nm. The source and optics yield axial and lateral resolutions of approximately 2.3μm and 3.9 μm resolution, respectively. The OCT sample fiber and the SMC fiber bundle are epoxied to a spacer, GRIN lens, annulus and right angle prism to achieve side-viewing SMC and OCT. The optics assembly is free to rotate and translate within a glass envelope with an outer diameter of 2.3 mm.

Animals

Twenty-five female A/J mice (age 5 weeks, Harlan Laboratories, Madison WI) were housed in the University of Arizona Animal Care facilities, and treated under protocols approved by the University of Arizona Institutional Animal Care and Use Committee. Mice were allowed to acclimate for one week, then were injected with either 0.2ml of USP grade saline (9 mice), or 10mg/kg by weight azoxymethane (AOM) (Sigma-Aldrich Chemicals, St. Louis, MO) (16 mice), subcutaneously once a week for 5 weeks. Two weeks prior to imaging, mice were placed on a chlorophyll free diet (AIN-93G, Harlan Laboratories, Madison WI) to remove potential background fluorescence from chow. Table 1 provides an overview of the studies performed and the number of animals per study.

24 hours before imaging, mice were fasted and given a pediatric electrolyte solution. Immediately prior to imaging, mice were anesthetized with a ketamine/xylazine mix (80–100mg/kg ketamine + 10mg/kg xylazine). The colon was flushed with approximately 3 cc warm saline before the introduction of 1% solution of N-acetlycysteine (Sigma-Aldrich, St. Louis, MO). After two minutes, the colon was again flushed with saline before a lavage of 0.2ml of 1% methylene blue solution. After three minutes a final saline flush was used to remove excess methylene blue. Prior to use, the methylene blue solution was sterile filtered to remove aggregates.

Imaging

The anesthetized mouse was placed on a heated pad and a sterile ocular gel placed on the eyes to prevent drying. The endoscope was coated with a water-based lubricant and inserted 30mm inside the colon. Three hundred and twenty overlapping SMC images were obtained in each 30mm longitudinal scan. For full imaging of the surface of the distal 30mm of colon, eighteen rotations were obtained. In saline mice, only ventral and dorsal rotations were imaged. For OCT, 30mm long cross-sectional images were obtained at either 8 rotations or only the ventral and dorsal rotations, to sample the colon. Due to a fiber breakage, a second endoscope with the same resolution and form factor was used for some OCT imaging in the study. All proximal optics (from the coupler to detection) remained the unchanged throughout the study.

Three studies were performed in all (Table 1). Two acute studies were performed: the methylene blue acute study and the AOM acute study. The methylene blue study utilized nine saline treated mice imaged only once at 30–36 weeks of age. Mice underwent the colon preparation and staining process described above, then SMC and OCT images were obtained at the ventral and dorsal rotations. Mice were imaged and euthanized at the following time points after staining: immediately (two mice), 15 minutes (one mouse), 30 minutes (three mice), 45 minutes (one mouse), and 60 minutes (2 mice).

For the AOM acute study, ten AOM-treated mice were imaged only once, at the following ages: 20 weeks (1 mouse), 28 weeks (3 mice), 30 weeks (2 mice), 32 weeks (3 mice), and 36 weeks (1 mouse) of age, then were euthanized.

The third study was a longitudinal study, imaging six AOM-treated mice approximately every four weeks beginning at 12 weeks of age (2 weeks after the end of AOM treatments)

until 30–36 weeks of age. After imaging for intermediate time points, mice were allowed to recover from anesthesia before returning to Animal Care. After the final imaging time point, mice were euthanized.

Explant and Histology

After euthanasia, the distal 30mm of the colon was explanted and opened longitudinally. For the methylene blue acute study (9 saline treated mice), the colons were snap frozen in optimum cutting temperature compound. The colons were cross-sectionally cryosectioned into 5μm sections. Sections from the dorsal and ventral rotations were imaged for methylene blue fluorescence with a fluorescence microscope (IX70, Olympus, Minneapolis, MN). After fluorescence imaging, the colons were stained with the high iron diamine-Alcian blue and imaged with the reflectance microscope (BX41, Olympus, Minneapolis, MN) to identify the presence of mucus.

For all 16 AOM-treated mouse colons, *ex vivo* imaging was performed with the SMC modality at selected normal and diseased regions of the colon, for comparison with *in vivo* images. Additionally, three other images were obtained: a gross image taken with a compact camera to document locations of adenoma, a fluorescence image obtained with a tabletop top surgical microscope (MVX10, Olympus, Minneapolis, MN) with Cy5 filter cube to image methylene blue fluorescence, and a white light microscopy image (BX41, Olympus, Minneapolis, MN) to show methylene blue absorption and confirm disease seen in the gross images.

After *ex vivo* imaging, the colons were fixed with 10% buffered formalin. This tissue was paraffin embedded and sectioned *en face* to create slides of the same orientation as was imaged by SMC *ex vivo*. Six μm thick sections were collected every 50μm and were stained with H&E.

Image Preprocessing—For visualization purposes, local histogram equalization utilizing the CLAHE function in Fiji (NIH, Bethesda, MD) was performed on all SMC images. This processing step reduced the effect of non-uniform illumination and transmission efficiency across the SMC field of view. For quantitative analysis, such as the SMC maps described below, no equalization was performed. OCT images were displayed in logarithmic intensity scale and 2×2 pixel median filter performed to reduce noise.

Three maps of the colon were created by utilizing SMC, OCT and gross/histological/ microscopic image data. The vertical axis of the map is the circumferential axis of the colon, and the horizontal axis of the map is the longitudinal axis of the colon. To create the SMC map, the average intensity of each SMC image was calculated using Matlab (The Mathworks, Natick, MA). A map with the same number of elements as SMC images was created, with dimension of 18 in the circumferential axis and 320 in the longitudinal axis. The most distal 50 elements at each of the 18 rotations, corresponding to the 4 mm closest to the anus, were removed because of strong fluorescence from methylene blue on the fur. The resulting 18×270 element map was then resampled to an 8×15 element map by bicubic interpolation in Matlab.

OCT maps were created from the 30mm longitudinal images obtained at 8 rotations. Each OCT image was divided into 2mm sections, creating an 8×15 element map. Tumors were identified in the OCT image as areas exhibiting increased signal attenuation, faint to obscured tissue boundary, mucosal thickening, and a signal void dip surrounding a protrusion (criteria previously established in our lab [Hariri 2007]). OCT map elements corresponding to a tumor were marked with a “1” and areas without tumor with a “0”.

Finally, gross image maps were created from the gross tissue photographs. Using ImageJ (NIH, Bethesda, MD) and the calibration rulers photographed with the tissue, an 8×15 element grid was sized to the gross images. Gross image map elements containing adenoma (as confirmed by histology and microscopy) were marked with a “1”. Other elements were marked with a “0”.

Comparison of OCT, gross, and SMC image maps—OCT and gross image maps were compared to ascertain the accuracy of OCT. An element filled by a “1” (tumor) in the OCT image map was considered a true positive if it was within 2 elements in the longitudinal axis, and 1 element in the rotational axis, of a “1” in the gross image map. Otherwise it was considered a false positive. A false negative was counted if there was no “1” in the OCT image within the tolerances stated above, of a “1” in the gross image map. The position tolerances were allowed because the colon is highly elastic, and the apparent location of tumors *in vivo* with an inserted endoscope may vary from locations measured on an explanted and opened colon.

To compare OCT and SMC image maps, a variable threshold was applied to each SMC map. At each threshold, regions of superthreshold intensity in the SMC map with a corresponding OCT map element of “1” (tumor) were counted as true positives. Regions of subthreshold SMC map intensity and “0” in the OCT map were counted as true negatives. As both modalities were endoscopic, no position tolerance was allowed. Sensitivity and specificity were calculated at each threshold and used to create receiver operating characteristic (ROC) curves, and the area under the curve (AUC) computed.

Human Observer Study—Eighty *in vivo* SMC images were selected to use in a human observer study. One-half of the images were obtained from saline mice (“normal”) and one-half from AOM-treated mice (“abnormal,” including approximately equal numbers of images obtained from regions without a tumor, small-moderate sized tumors, and large tumors). Images were selected that were absent of artifacts and exhibited high contrast. Twenty of these images were randomly chosen and used as a training set. The remaining 60 images were shown to five naïve observers in a random order. Observers were asked to give a diagnosis normal or abnormal on a five point confidence rating scale (1 - disease definitely absent, 2 – disease probably absent, 3 – disease possibly present, 4 – disease probably present, and 5 – disease definitely present). Sensitivity and specificity to disease was computed at each confidence rating threshold. The area under the ROC curve was calculated using the perfcurve function in Matlab.

Results

All saline mice were successfully imaged and analyzed. All AOM mice but one developed adenoma in the distal colon. One mouse from the AOM acute study was euthanized due to a severe abscess, and poor histology was obtained on 3 mice, so data from only 6 of the AOM acute study mice were analyzed. All six AOM mice completed the longitudinal study and were included in the analysis.

Saline Mice – Methylene Blue Acute Study

Results from the study of the methylene blue contrast agent in saline-treated mice showed that there was a moderate time window available for high contrast imaging. For the first 30 minutes, excellent contrast was observed in fluorescence microscopy images of colon cryosections, showing strong fluorescence emission signal from the contrast agent. However, a loss of both signal strength and contrast was noted over the course of 60 minutes, as shown in Figure 1. Panel A shows the fluorescence microscope image for a cryosection obtained from a mouse that was euthanized immediately after contrast agent lavage and imaging. Fluorescence signal from the methylene blue is evident in the crypts and strongest at the surface. Strong, localized signal from the mucosa was lost in mice euthanized after 30 minutes and a low, more diffuse level of signal was maintained through 60 minutes. Histological sections stained with high iron diamine-Alcian blue agent showed minimal mucus accumulation on the surface of the colon, suggesting that mucus return was not causing the loss of contrast (data not shown). The small sections of mucus observed appeared to be areas that were not removed by N-acetlycysteine lavage, but these areas generally exhibited good methylene blue staining regardless.

Ex vivo results mirrored those seen *in vivo*. High contrast images of colonic crypt patterns were obtained for approximately 30 minutes after methylene blue lavage. After that time, image signal and contrast was lower, excepting that large tumors were visible with high contrast due to the presence of irregular regions of high signal.

Saline and AOM Mice Acute Studies

In vivo SMC images of non-tumor colon tissue exhibited two specific patterns; honeycomb and dot, shown in Figure 2. These patterns arise from the uptake and subsequent fluorescence emission of methylene blue: the honeycomb is a series of connected lines with a dark center, whereas the dot pattern is a set of disconnected disks of signal. In the *en face* images exhibiting the honeycomb pattern, crypt lumens appear black in SMC and white in reflectance images. For the dot pattern the contrast is reversed: crypt lumens are white in SMC and blue in reflectance images. Figure 2 shows example images of each type of pattern, in both saline and AOM treated mice. Honeycomb pattern images are shown in the top row and dot pattern images on the bottom row. Saline mice are in the left column and AOM-treated mice on the right. It can be noted that images of the saline mice exhibit a very regular pattern, with honeycomb or dots of approximately equal size and spacing, and consistent contrast, across the field of view. In contrast, images of the AOM mouse colon shows irregular organization; the honeycomb is distorted, dot size varies, and contrast is uneven across the field of view.

Figure 3 shows *ex vivo* images of the honeycomb (top row) and dot pattern (bottom row) from AOM-treated mice. It can be noted that the fluorescence in SMC images (left column), corresponds to methylene blue staining, shown in reflected light images (middle column), and crypt walls (honeycomb pattern) or lumens (dot pattern) seen in histology (right column). Both SMC images demonstrate irregularity. Histological comparison shows irregularities in lumen size and wall thickness, as well as abnormally large lumen size in the dot pattern colon suggesting that while these colons do not represent neoplastic tissue; neither do they represent normal tissue. These patterns are similar to type II (non-neoplastic, hyperplastic) pits, which can be asteroid or onion-like but arranged similarly to normal crypts (25).

Figure 4 shows representative *ex vivo* SMC, reflectance, and H&E stained histology images of adenoma in AOM acute study mice. Images of a small adenoma, around 1mm in diameter (Fig. 4A–C) and a large adenoma, over 2mm diameter, (Fig. 4D–F) are shown. The SMC image of the small adenoma shows a highly irregular pattern with some resemblance to the honeycomb pattern. White light images reveal thickened crypt walls and abnormal lumens - typically elliptical- with increased size. This description agrees with Kudo's pit pattern group type III (25). Histology exhibits the same elongated and disorganized crypts and confirms the presence of adenoma. SMC images of the large adenoma exhibit signal level and pattern discontinuity across the field of view. The reflectance image shows that the methylene blue formed aggregates on a diffuse blue background, with no apparent crypts. These images exemplify the type V pit pattern: the mucosa is devoid of pits (25), although some structure remains beneath the surface as shown in in the histology image.

A representative set of data obtained from SMC, OCT, and gross images is shown in Figure 5. Tumors on the gross image are clearly visualized by OCT and are represented as red blocks (value of "1") in the OCT image map. These regions of OCT-identified tumors visually show good correlation to regions of high intensity visualized on the SMC map. A quantitative comparison of the OCT and SMC maps, using a variable SMC intensity threshold, reveals an AUC for this mouse of 0.75. For all mice, the mean area under the ROC curve was 0.60 with a standard deviation of 0.19, indicating only a low correlation between regions of OCT-identified tumors and high SMC image fluorescence intensity.

The human observer study showed that the differentiation between normal and abnormal colon is possible using SMC images. For the 5 observers, the computed AUCs ranged from . 83 to .92, with an average of .87. For the top-performing observer, a sensitivity to abnormality of 100% was obtained at a specificity of 83%. Small and large adenoma were identified correctly 100% of the time.

AOM Mice Longitudinal Study

A representative time course of OCT (left column) and SMC (right column) images is shown in Figure 6. Cross-sectional OCT images are 6mm longitudinal, cropped from the 30 mm longitudinal image taken at the ventral rotation, centered 15mm proximal from the anus. The colon lumen is at the top of the images. *En face* SMC images are 720μm diameter and are obtained of the luminal surface at the center of the OCT images. The first time series images were taken two weeks after AOM injections ended. The colon appears grossly

normal in the OCT image. The layers of the colon (mucosa, submucosa, and muscle layers) are visible and the colon surface is smooth, making contact with the endoscope envelope. However, the SMC shows some distortion in the honeycomb pattern suggesting some early abnormality. The time point 2 OCT image reveals the beginning of tumor development; shown as mild thickening of the mucosa and increased signal attenuation at the boundary between mucosa and submucosa in the center of the OCT image. Increasingly irregular crypt organization is seen in the SMC image. The OCT image of time point 3 shows an adenoma according to defined criteria; local mucosal thickening, increased signal attenuation, an obscured boundary between the mucosa and submucosa, and presence of the characteristic dip surrounding a protruding tumor. The SMC image shows diffuse fluorescence, spotted with intense regions. Signal was only visible directly on top of the adenoma, where the colon was making contact with the probe. The tumor has grown in the final time point, shown clearly in the OCT image. The SMC image shows an increase in the number of methylene blue aggregates, visible as irregular bright regions. A white light image confirms that methylene blue has aggregated at the edge of the tumor and histology confirms an adenoma (Figure 7).

Discussion

OCT and fluorescence-based SMC are complementary modalities capable of screening the colon for early events in carcinogenesis. OCT can easily and quickly assess the overall health of the colon by imaging mucosa thickness, whether boundaries are visible, and visualizing the presence and size of protruding adenoma. SMC can image crypt patterns and appears to be sensitive to abnormalities before they are visible on OCT images.

SMC imaging using the FDA-approved contrast agent methylene blue in fluorescence mode was highly successful. However, only a limited time window (approximately 30 minutes) was available for imaging after the contrast agent lavage. Prior lavage with a mucolytic agent was critical to remove most mucus, which improved contrast agent uptake and image quality. Mucus did not return after 30 minutes, which suggests that it is not the cause of the loss of contrast over time. We conclude therefore, because of the decrease in surface staining, that the methylene blue, as a dye absorbed in the mucosa, is being removed from the lumen of the colon through regular clearance mechanisms. Imaging either needs to be completed within this time frame, or an alternative application method employed. For example, the methylene blue could be sprayed on the colon in segments, as is done in human colonoscopies, and rinsed during an endoscopic visualization procedure (26).

SMC images revealed two characteristic patterns in non-tumor tissue, the honeycomb and the dot. Both patterns were seen in saline (control) mice, so there was no correlation between pattern type and tissue abnormality, and it is unclear why the two patterns were seen. It is clear from the comparison of saline mice to AOM- treated mice that AOM has an effect on the entire colon, suggesting an inflammatory and disruptive process. It may be that the observed abnormalities in the honeycomb and dot patterns are the first signs of disease, a field cancerization effect, or a unique effect of AOM treatment (27). It is promising that the SMC modality is sensitive to these changes, which occur before abnormalities appear in OCT or gross images.

Similar to the ‘dip’ effect seen in OCT images of adenoma (due to the colon being pushed away from the envelope of the endoscope by the protruding adenoma), SMC images of adenoma typically appeared as regions of increased fluorescence over the tumor, surrounded by regions with limited signal, since the tissue was not in contact with the endoscope. Directly on top of the adenoma, there was a spectrum of appearances; in small adenoma crypts appeared highly irregular or disconnected from the surrounding areas, and regions were sometimes visualized with elongated crypts. In larger adenoma, regions with hyperintense punctate signal or no clear structure were seen. Examination of histology revealed that smaller and flatter adenoma have disrupted and/or elongated crypts, whereas large adenoma protruding into the lumen were had areas devoid of discernible crypt pattern. These findings are consistent with previously reported chromoendoscopy studies(25, 28, 29).

Because we observed that regions of thickened epithelium on OCT images were often associated with increased fluorescence due to increased methylene blue dye absorption in the early stages of disease, and since hyperintense regions of fluorescence from methylene blue aggregate were seen on many large tumors, it was expected that the average intensity of the SMC signal might be correlated with disease. However, the average AUC of the ROC curves was only 0.60, suggesting only a low correlation. In some mice the correlation was no better than chance. This could be indicative of a spectrum of staining, early hyperplastic events could exhibit increased methylene blue staining (30) but as disease progresses and inflammation and adenomas form, removing normal functioning cells, methylene blue uptake diminishes (31, 32). However, human observers were able to distinguish normal from abnormal colon with excellent accuracy (average AUC of the ROC curves of nearly 0.9). These findings suggest that the SMC modality is best utilized in imaging mode for detecting early cancerous changes. Some confounders in SMC images included fluid, blood, and feces. However, these items were easily identified on OCT images. Lymphoid aggregates were associated with low SMC fluorescence intensity, but again these structures were easily identified on OCT images. OCT can detect adenoma with high sensitivity and low false positive rate (21) suggesting that OCT is the more appropriate modality for visualizing more advanced disease. For small adenoma, both the changes in crypt pattern seen in SMC images and the alterations in tissue microstructure seen in OCT are useful.

The dual modality endoscopic system permits early detection of neoplastic events with SMC, as well as tracking of number and size of adenoma with OCT. Unlike forward-viewing endoscopes which require insufflation and skilled users to examine the colon walls (33), this system is capable of automated, methodical interrogation, without insufflation, of the entire distal colon and requires minimal training. The dual modality system is sensitive to the dysregulation in crypt pattern – shown in the comparison of saline to AOM mice as well as in early stage adenoma. Demonstrated here is imaging of the structure of the colon with the FDA-approved nonspecific dye methylene blue, but the system can also be used with targeted dyes in order to map the molecular expression of the tissue in a time serial fashion, making the dual-modality endoscope a flexible platform for understanding colon cancer development, and potentially, future clinical diagnostics.

Acknowledgments

Funding:

NIH R01 CA109835

NIH Graduate Training in Biomedical Imaging and Spectroscopy T32EB000810

References

1. American Cancer Society. Cancer Facts and Figures. Atlanta, GA: American Cancer Society; 2014. http://www.cancer.org/acs/groups/content/@research/documents/webcontent/acspc-042151.pdf,
2. Wallace MB, Kiesslich R. Advances in Endoscopic Imaging of Colorectal Neoplasia. Gastroenterology. 2010 May; 138(6):2140–2150. [PubMed: 20420951]
3. Van Rijn JC, Reitsma JB, Stoker J, Bossuyt PM, van Deventer SJ, Dekker E. Polyp Miss Rate Determined by Tandem Colonoscopy: A Systematic Review. Am J Gastroenterol. 2006 Feb; 101(2):343–350. [PubMed: 16454841]
4. Taketo MM, Edelmann W. Mouse Models of Colon Cancer. Gastroenterology. 2009 Mar; 136(3): 780–798. [PubMed: 19263594]
5. Corpet DE, Pierre F. Point: From Animal Models to Prevention of Colon Cancer. Systematic Review of Chemoprevention in Min Mice and Choice of the Model System. Cancer Epidemiol Biomarkers Prev. 2003 May 1; 12(5):391–400. [PubMed: 12750232]
6. Gerner, EW.; Ignatenko, NA.; Besselsen, DG. Preclinical Models for Chemoprevention of Colon Cancer. In: Senn, PDH-J.; Morant, DR., editors. Tumor Prevention and Genetics [Internet]. Berlin Heidelberg: Springer; 2003. p. 58-71.Available from: http://link.springer.com/chapter/10.1007/978-3-642-55647-0_6 [cited 2014 May 5]
7. Huang EH, Carter JJ, Whelan RL, Liu YH, Rosenberg JO, Rotterdam H, et al. Colonoscopy in Mice. Surg Endosc Interv Tech. 2002 Jan 1; 16(1):22–24.
8. Becker C, Fantini MC, Neurath MF. High resolution colonoscopy in live mice. Nat Protoc. 2007 Jan; 1(6):2900–2904. [PubMed: 17406549]
9. Durkee BY, Shinki K, Newton MA, Iverson CE, Weichert JP, Dove WF, et al. Longitudinal Assessment of Colonic Tumor Fate in Mice by Computed Tomography and Optical Colonoscopy. Acad Radiol. 2009 Dec.16(12):1475–1482. [PubMed: 19896065]
10. Fennerty MB. Tissue staining (chromoscopy) of the gastrointestinal tract. Can J Gastroenterol J Can Gastroenterol. 1999 Jun; 13(5):423–429.
11. Eisen GM, Kim CY, Fleischer DE, Kozarek RA, Carr-Locke DL, Li TCM, et al. High-resolution chromoendoscopy for classifying colonic polyps: A multicenter study. Gastrointest Endosc. 2002 May; 55(6):687–694. [PubMed: 11979251]
12. Kiesslich R, Fritsch J, Holtmann M, Koehler HH, Stolte M, Kanzler S, et al. Methylene blue-aided chromoendoscopy for the detection of intraepithelial neoplasia and colon cancer in ulcerative colitis. Gastroenterology. 2003 Apr; 124(4):880–888. [PubMed: 12671882]
13. Kiesslich R, Neurath MF. Magnifying chromoendoscopy for the detection of premalignant gastrointestinal lesions. Best Pract Res Clin Gastroenterol. 2006 Feb; 20(1):59–78. [PubMed: 16473801]
14. Bird, RP. Aberrant Crypt Foci System to Study Cancer Preventive Agents in the Colon. In: Hanausek, M.; Walaszek, Z., editors. Tumor Marker Protocols [Internet]. New York: Springer; 1998. p. 465-474.Available from: http://link.springer.com/protocol/10.1385/0-89603-380-5%3A465 [cited 2014 May 5]
15. Takayama T, Katsuki S, Takahashi Y, Ohi M, Nojiri S, Sakamaki S, et al. Aberrant Crypt Foci of the Colon as Precursors of Adenoma and Cancer. N Engl J Med. 1998; 339(18):1277–1284. [PubMed: 9791143]
16. Kudo S, Tamura S, Nakajima T, Yamano H, Kusaka H, Watanabe H. Diagnosis of colorectal tumorous lesions by magnifying endoscopy. Gastrointest Endosc. 1996 Jul; 44(1):8–14. [PubMed: 8836710]

17. Wada Y, Kashida H, Kudo S, Misawa M, Ikehara N, Hamatani S. Diagnostic Accuracy of Pit Pattern and Vascular Pattern Analyses in Colorectal Lesions. Dig Endosc. 2010 Jul 1; 22(3):192–199. [PubMed: 20642608]
18. Kobayashi Y, Kudo S, Miyachi H, Hosoya T, Ikehara N, Ohtsuka K, et al. Clinical usefulness of pit patterns for detecting colonic lesions requiring surgical treatment. Int J Colorectal Dis. 2011 Dec 1; 26(12):1531–1540. [PubMed: 21607587]
19. Kiesslich R, Goetz M, Hoffman A, Galle PR. New imaging techniques and opportunities in endoscopy. Nat Rev Gastroenterol Hepatol. 2011 Oct; 8(10):547–553. [PubMed: 21894196]
20. Vakoc BJ, Fukumura D, Jain RK, Bouma BE. Cancer imaging by optical coherence tomography: preclinical progress and clinical potential. Nat Rev Cancer. 2012 May; 12(5):363–368. [PubMed: 22475930]
21. Hariri, LP.; Qiu, Z.; Tumlinson, AR.; Besselsen, DG.; Gerner, EW.; Ignatenko, N., et al. [cited 2014 May 5] Serial endoscopy in azoxymethane treated mice using ultra-high-resolution optical coherence tomography. 2007. p. 643208–643208–10Available from: http://dx.doi.org/10.1117/12.699249.
22. Adler DC, Zhou C, Tsai T-H, Schmitt J, Huang Q, Mashimo H, et al. Three-dimensional endomicroscopy of the human colon using optical coherence tomography. Opt Express. 2009 Jan 19; 17(2):784–796. [PubMed: 19158891]
23. Wall RA, Barton JK. Fluorescence-based surface magnifying chromoendoscopy and optical coherence tomography endoscope. J Biomed Opt. 2012; 17(8):0860031–0860037.
24. Winkler AM, Rice PFS, Drezek RA, Barton JK. Quantitative tool for rapid disease mapping using optical coherence tomography images of azoxymethane-treated mouse colon. J Biomed Opt. 2010; 15(4):041512–041512–10. [PubMed: 20799790]
25. Kudo S, Rubino C, Teixeira C, Kashida H, Kogure E. Pit Pattern in Colorectal Neoplasia: Endoscopic Magnifying View. Endoscopy. 2004 Oct 25; 33(04):367–373. [PubMed: 11315901]
26. ASGE Technology Committee. Chromoendoscopy. Gastrointest Endosc. 2007; 66(4):639–649. [PubMed: 17643437]
27. Chen J, Huang X-F. The signal pathways in azoxymethane-induced colon cancer and preventive implications. Cancer Biol Ther. 2009 Jul 15; 8(14):1313–1317. [PubMed: 19502780]
28. Devuni D, Vaziri H, Anderson Joseph C. Chromoscolonoscopy. Gastroenterol Clin N Am. 2013; 42:521–545.
29. Togashi K, Konishi F. Magnification chromo-colonoscopy. ANZ J Surg. 2006 Dec; 76(12):1101–1105. [PubMed: 17199698]
30. Bird RP. Observation and quantification of aberrant crypts in the murine colon treated with a colon carcinogen: Preliminary findings. Cancer Lett. 1987 Oct 30; 37(2):147–151. [PubMed: 3677050]
31. Trivedi PJ, Braden B. Indications, stains and techniques in chromoendoscopy. QJM Mon J Assoc Physicians. 2013 Feb; 106(2):117–131.
32. Canto MI. Vital staining and Barrett's esophagus. Gastrointest Endosc. 1999 Mar; 49 Supplement(3):S12–S16. [PubMed: 10049441]
33. Rex DK. Optimal Withdrawal and Examination in Colonoscopy. Gastroenterol Clin North Am. 2013 Sep; 42(3):429–442. [PubMed: 23931852]

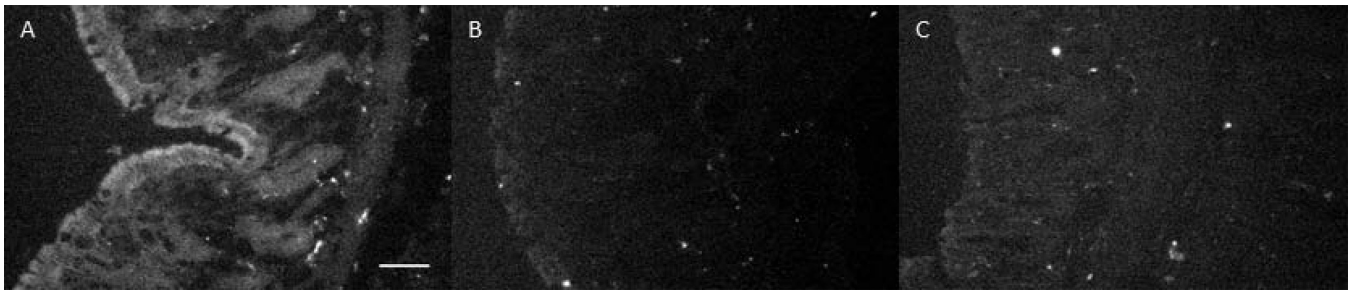

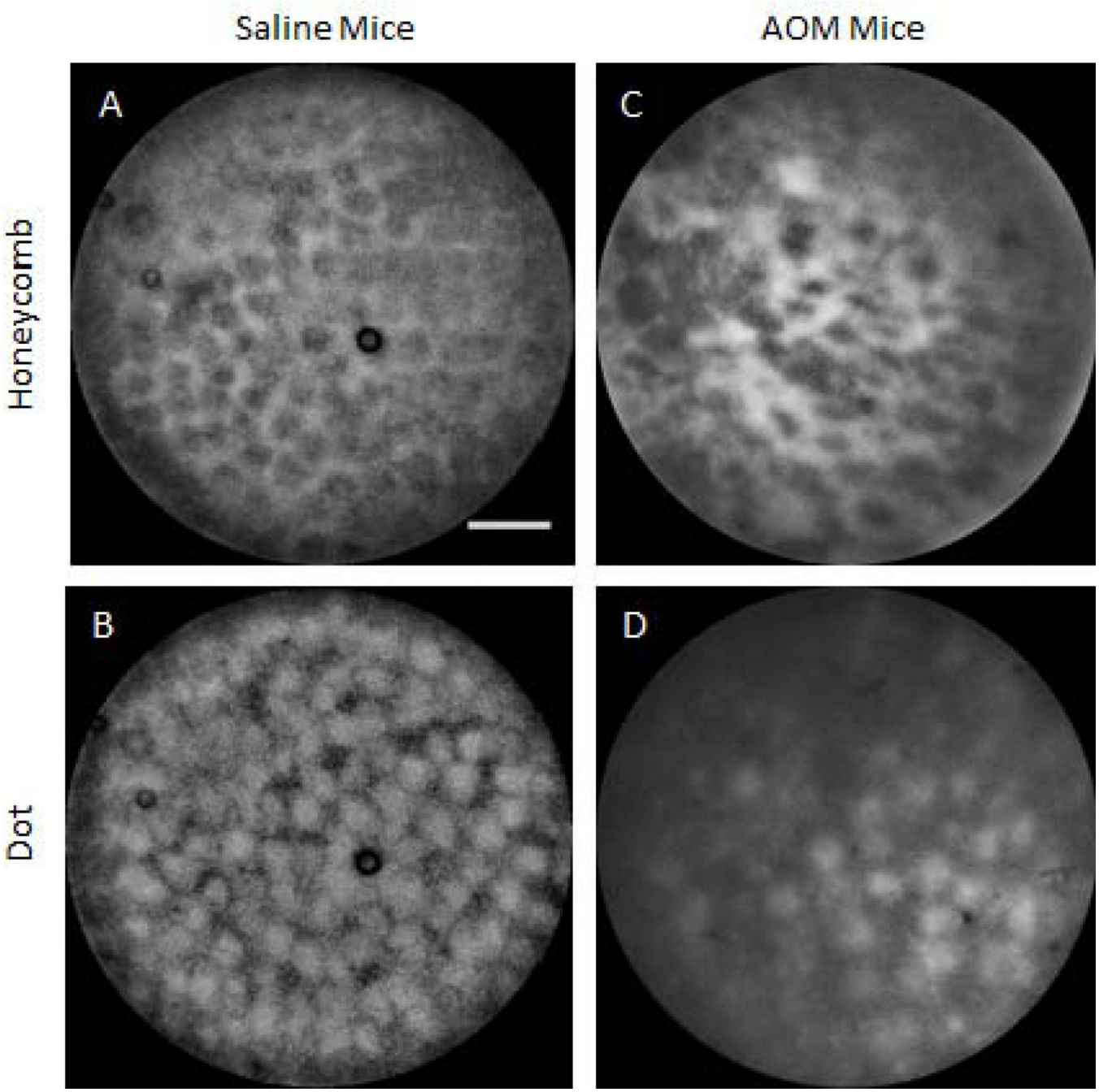

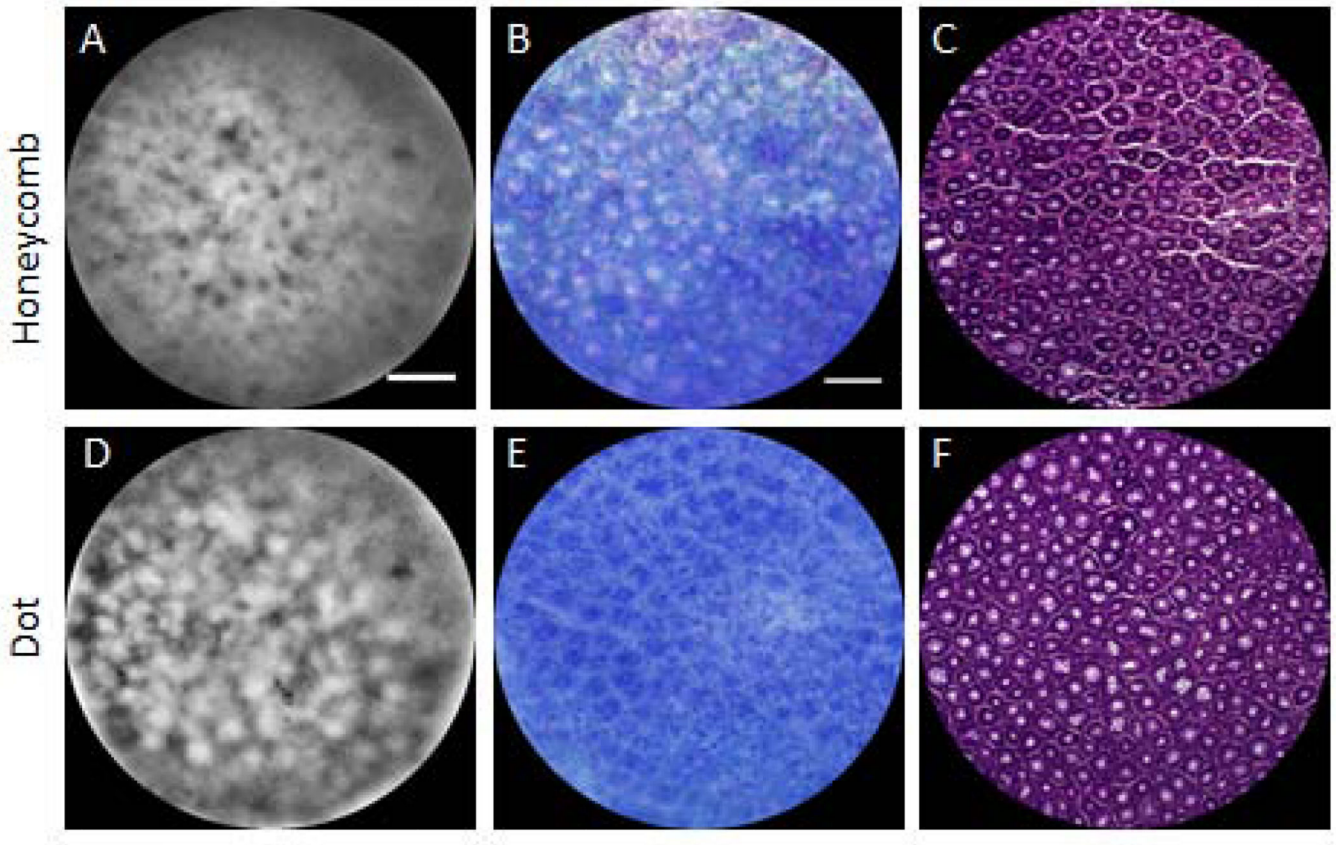

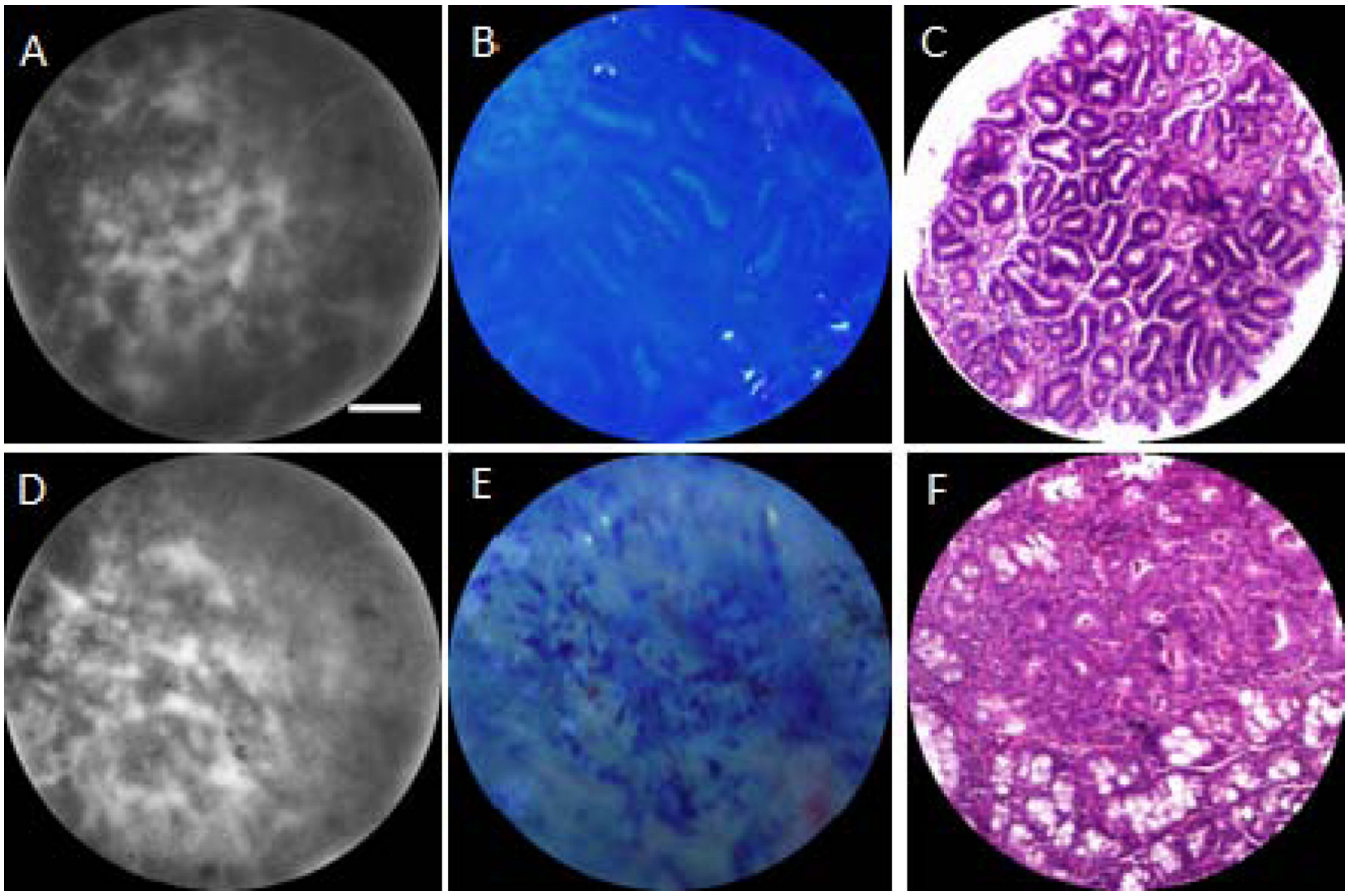

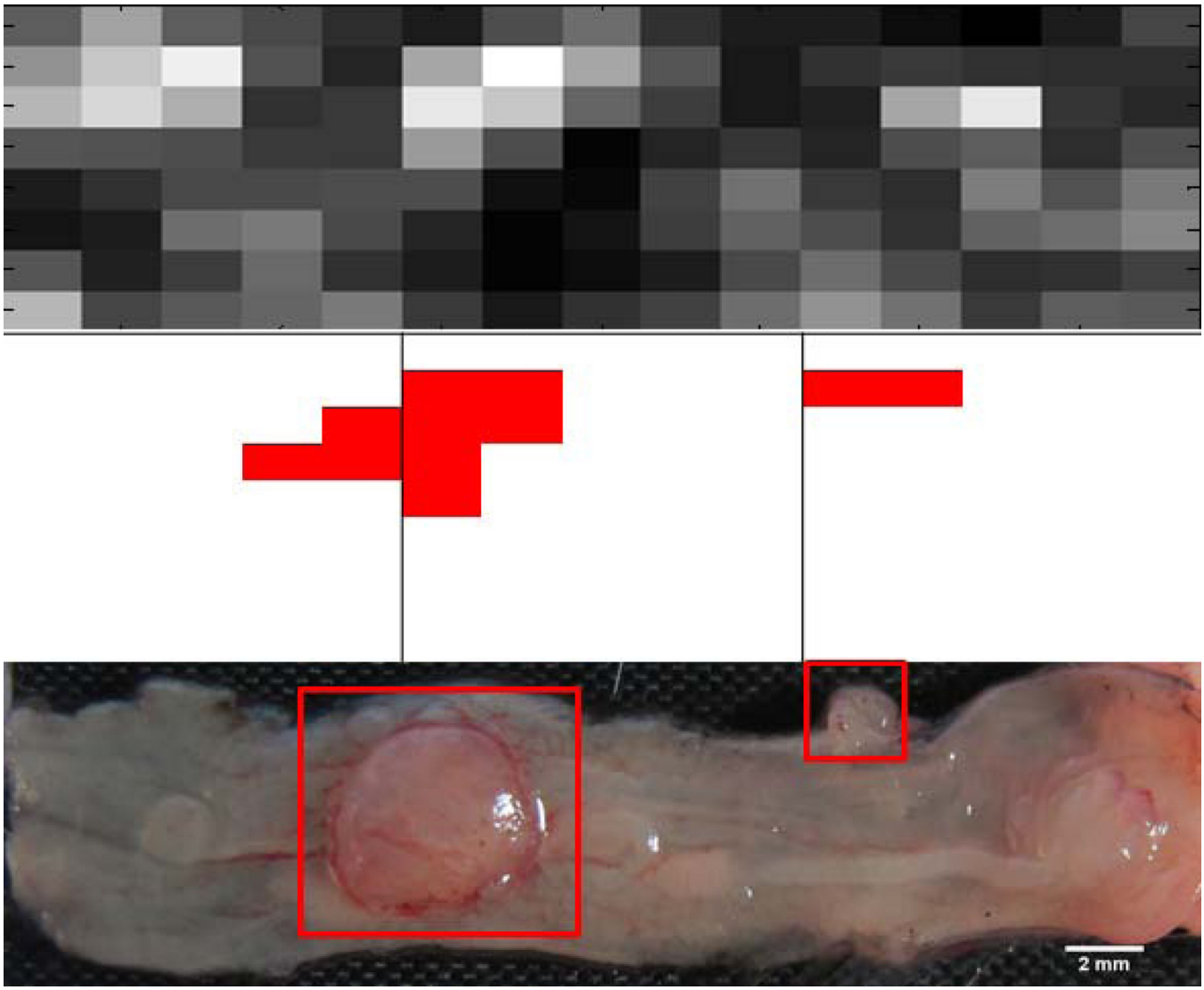

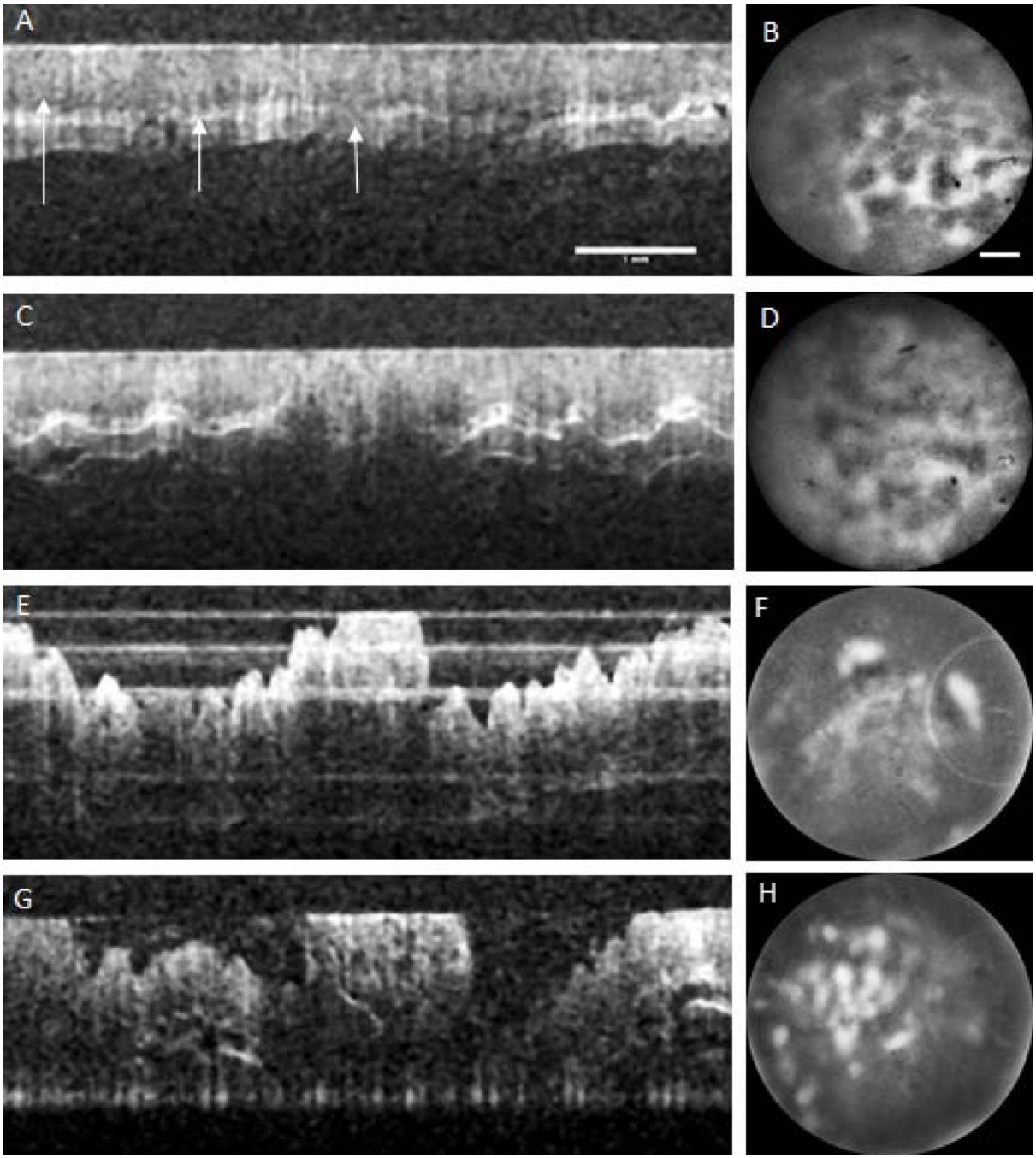

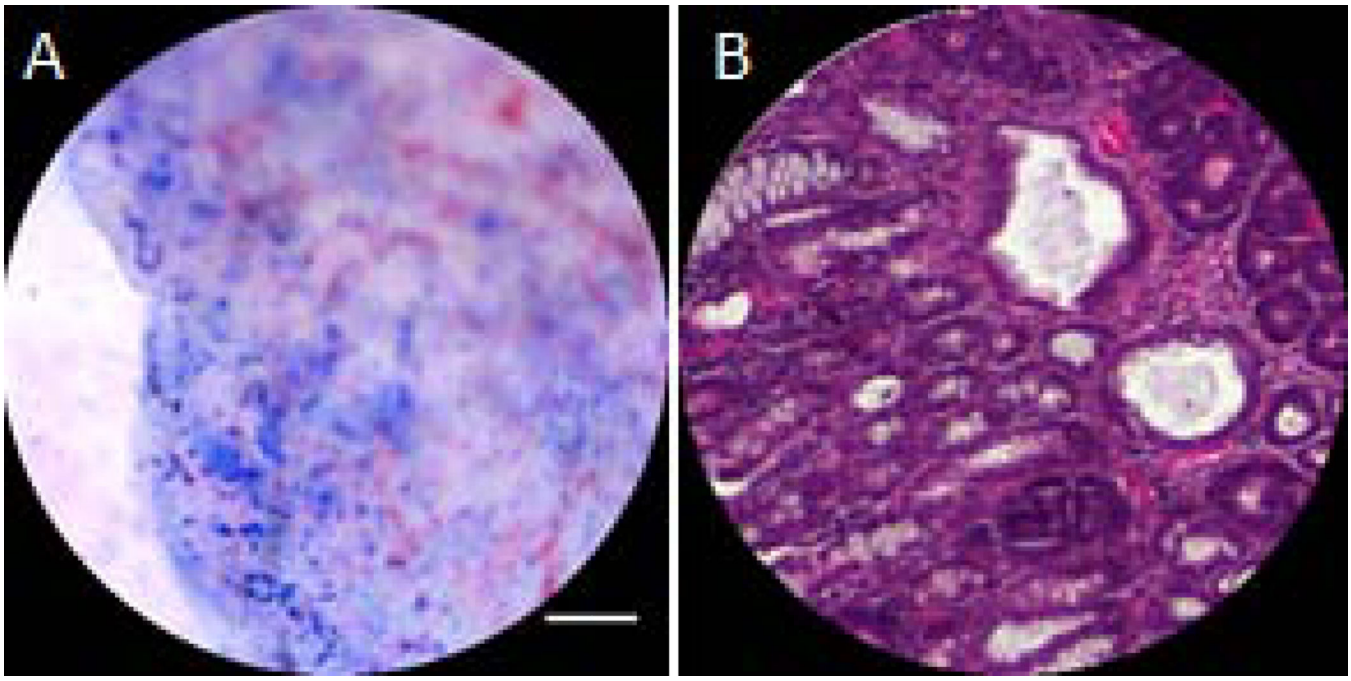

Table 1

Overview of studies performed.

25 A/J Mice		
9 Saline mice Given USP saline injections subcutaneously once a week for 5 weeks	**16 AOM mice** Given AOM injections subcutaneously once a week for 5 weeks	
Methylene Blue Acute: 9 mice imaged and euthanized at 36 weeks of age	**AOM Acute:** 10 mice imaged and euthanized between 30 to 36 weeks of age	**Longitudinal:** 6 mice imaged every 4 weeks beginning at 12 weeks and euthanized between 30 and 36 weeks of age